A Preliminary Investigation on Selective Laser Melting of M2 High Speed Steel

Z.H. Liu, C.K. Chua & K.F. Leong
Nanyang Technological University, Singapore

K. Kempen, L. Thijs, E. Yasa, J.Van-Humbeeck & J.P. Kruth
Katholieke Universiteit Leuven, Belgium

ABSTRACT: Selective Laser Melting (SLM) is an Additive Manufacturing (AM) technique that is able to process both metallic and ceramic materials in powder form. The main attraction of SLM is the ability to produce near fully dense functional parts with high geometrical complexity. Parts can be fabricated with features and designs conventional manufacturing methods cannot achieve. In this study, the feasibility of processing M2 High Speed Steel (HSS) with the SLM technique is investigated. The main focus is on understanding the material properties to facilitate the optimization of process parameters in order to produce parts with good quality and high density. Laser powers of 90 W and 105 W were used with scan speeds ranging from 100 mm/s to 850 mm/s. Preliminary results show that parts exhibit warpage, cracking and partial separation from the base plate. In addition, the degree of cracking and base plate separation is more pronounced at lower scan speeds. While residual stresses mainly accounted for the problems occurred in this study, in depth microstructural analysis might also explain the cracking at lower scan speeds. It was found that the microstructure was different for parts produced at different scan speeds, providing some insights on suitable processing parameters for the family of tool steels. In an attempt to reduce residual stresses, lower thermal gradient was achieved by preheating of the base plate to 180^{o}C. Indeed, cracking, warpage and base plate separation were greatly reduced upon close visual inspection. It was also found that the chances of parts separating from the base plate were lower for AISI 1085 steel than for M2 HSS base plates. In conclusion, this study showed that SLM of M2 HSS is feasible with preheating conditions.

1 INTRODUCTION

1.1 *Background*

SLM is a promising technique in the field of AM (Campbell 2009) as it can process relatively a wide range of materials ranging from metallic to ceramic powders compared to other AM techniques. The ability and flexibility to produce parts without the need to include fabrication and manufacturing post processes such as milling and turning also give rise to its popularity for many different applications in areas such as biomedical, automotive and aerospace (Kruth, *et al.* 2005; Wehmoller, *et al.* 2005; Mumtaz, *et al.* 2007; Shishkovsky, *et al.* 2007; Vandenbroucke, *et al.* 2007; Chua, *et al.* 2010).

Some commercialized materials that have proven to work with SLM include Titanium alloys ($TiAl_6V_4$, $TiAl_6Nb_7$ and cp-Titanium), Aluminum alloys ($AlSi_{10}Mg$, $AlSi_{12}$ and 6/7000 series), Stainless Steel (316L and a few other series), Inconel (718 and 625), and Cobalt Chrome (3DSystems 2011; ConceptLaser 2011; EOS 2011; Louvis, *et al.* 2011; MTTTechnologies 2011; PhenixSystems 2011). For ceramics (Bertrand, *et al.* 2007), examples include Alumina (Shishkovsky, *et al.* 2007), Alumina–Zirconium Zirconia and Yttria–Zirconia (Mumtaz, *et al.* 2007). The list of SLM materials continues to grow today as researchers explore into different materials such as Gold (Khan, *et al.* 2010), Copper and Magnesium alloys (Nga, *et al.* 2010; Nga, *et al.* 2011). The range of applications is therefore expected to increase with the growth of SLM materials' list.

1.2 *Objectives*

The main objective of this study is to investigate SLM of a hardenable carbon steel, M2 HSS. In this research, different SLM process parameters are investigated in an attempt to produce good quality parts with high density and retaining properties comparable to conventionally produced M2 HSS. Microstructural analysis and microhardness tests are also carried out to understand how different process parameters affect the resulting microstructure of the SLM M2 HSS part. This understanding will help to facilitate future studies on processing other tool steels with the SLM technique which is in line with the objective of this research.

2 EXPERIMENTAL

2.1 *Material*

The M2 HSS powder used in this research was bought from LPW Technology (UK) and is produced by the gas atomization process. Particle size is between 15 to 45 µm as stated in the data sheet provided by LPW. Tests carried out with LEICA QWin software algorithm based on pixel counts from Light Optical Microscope (LOM) pictures resulted in an average grain size of 27.7 µm. The cumulative frequency distribution of the powder is shown in Figure 1. Table 1 shows the composition of the M2 HSS in weight percentage provided by LPW Technology compared with the typical M2 HSS composition.

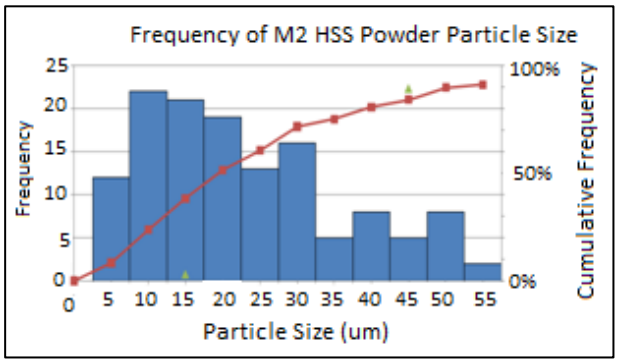

Figure 1. Cumulative frequency distribution of M2 HSS particles.

Table 1. Elemental composition of M2 HSS powder provided by LPW and compared with conventional M2 HSS composition.

Element	LPW	Conventional
	%	%
Carbon, C	0.9	0.78 – 0.88, 0.95 – 1.05
Silicon, Si	0.35	0.20 – 0.45
Manganese, Mn	0.38	0.15 – 0.40
Chromium, Cr	3.97	3.75 – 4.50
Molybdenum, Mo	4.89	4.50 – 5.50
Vanadium, V	1.82	1.75 – 2.20
Tungsten, W	6.15	5.50 – 6.75
Iron, Fe	Balance	Balance

A SEM picture of the powder shown in Figure 2 reveals that the particles are spherical in shape as expected from the gas atomization process. This will provide excellent powder flowability that is necessary for an ideal powder layer deposition, ensuring good part density and quality.

2.2 *Procedure*

2.2.1 *SLM machine and process parameters*

The SLM machine used for this experiment is M3 Linear, from Concept Laser. Two laser powers of 90 W and 105 W were used with varying laser scan speeds from 250 mm/s to 700 mm/s in a nitrogen atmosphere where remnant oxygen level was kept

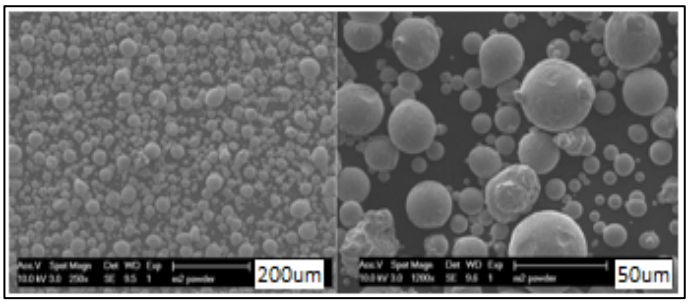

Figure 2. SEM of virgin M2 HSS powder.

less than 1%. For some SLM parts, laser remelting of each layer was applied to observe any improvements in surface roughness and part density. (Kruth, *et al.* 2008; Yasa, *et al.* 2009). It was found that better surface roughness and part densities were achieved when applying laser re-melting to AISI 316L Stainless Steel (SS) SLM parts. In the current research of M2 HSS, the laser re-melting was carried out with laser power 105 watt and scan speed 700 mm/s. As for scan spacings, values of a_1=62% (scan spacing between scan tracks), a_2=35% (specifying the distance of the first scan track to the island border) and a_3=50% (elongation of the scan tracks in one island) of the spot size were set. These scan spacings were optimized for 316L SS. Detailed information on scan spacing factors for the Concept Laser M3 Linear in island scanning for SLM is well documented in (Yasa, *et al.* 2010).

2.2.2 *Problems encountered*

There were some problems encountered during the processing of this material. The parts exhibited warpage, crackings and base plate separation. Furthermore, the degree of warpage, crackings and base plate separation was more pronounced in parts fabricated with low scan speeds. Figure 3 shows examples of cracking, warpage and base plate separation encountered. These problems seemed to suggest that high thermal stresses were induced during the process. Moreover, its high carbon content of 0.9% also results in high brittleness compared to AISI 316L SS and maraging 300 steel which have a carbon content of 0.03%.

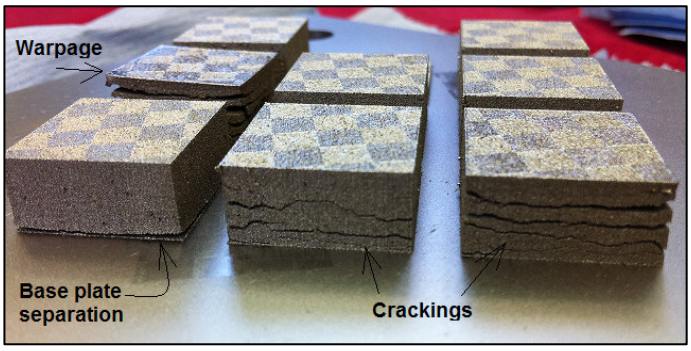

Figure 3. Parts showing crackings, base plate separation and warpage.

2.2.3 *Pre-heating*

In the literature on laser welding, it is mentioned that pre-heating is necessary for high carbon (above 0.6% carbon content) steels (Ion 2005). High amounts of carbon are trapped within a body-centered cubic (BCC) crystalline structure during very fast cooling rates forming matensitic structure (body-centred tetragonal BCT), containing tremendous amount of internal stresses (Totten, *et al.* 2002). As such, preheating is typically applied to reduce the tendencies of thermal shock and residual stresses (Dawes 1992; 1997). In view of this, SLM of M2 HSS adopted preheating of the base plate before the process. The base plate was heated to 100°C and 180°C in two separate experiments. It was clear that preheating of 180°C reduced the cracking, warpage and base plate separation issues greatly. Table 2 shows the ratings of part quality without (25°C) and with preheating (180°C) based on visual inspection.

Table 2. Comparison of part quality at 25°C and 180°C preheating, based on visual inspection.

Process	25°C	180°C
Parameters	(On a scale of 0 to 10, good to bad)	
90 watt, 250 mm/s	5	1
90 watt, 400 mm/s	5	0.5
90 watt, 550 mm/s	2	0
105 watt, 250 mm/s	8	1
105 watt, 400 mm/s	7	0
105 watt, 550 mm/s	5	0
105 watt, 700 mm/s	6	0
*105 watt, 700 mm/s	6	0

* With laser re-melting

It is observed that preheating improves the part quality by reducing the thermal stresses. Figure 4 shows the quality of parts produced with and without preheating.

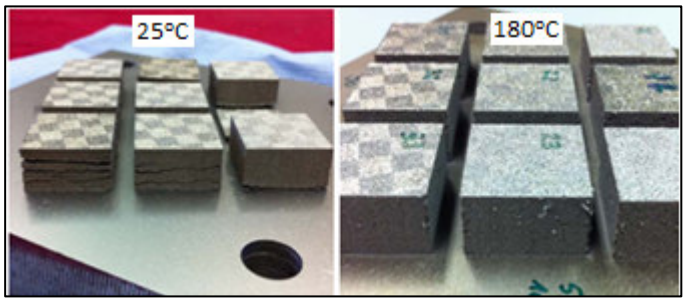

Figure 4. Parts produced with (right) and without (left) preheating.

3 RESULTS

3.1 *Density*

Using Archimedes principle (the absolute density value of M2 HSS used is 8.15 g/cm^3), it is found that good quality parts (without cracks) of density between 96% to 97% can be achieved with laser power of 105 W and laser scan speeds between 400 mm/s and 550 mm/s. While a scan speed of 250 mm/s might yield higher density parts, they possessed cracks all the time. Figure 5 shows the preliminary density results obtained. Scan speeds above 550 mm/s without re-melting produce parts with densities below 91%.

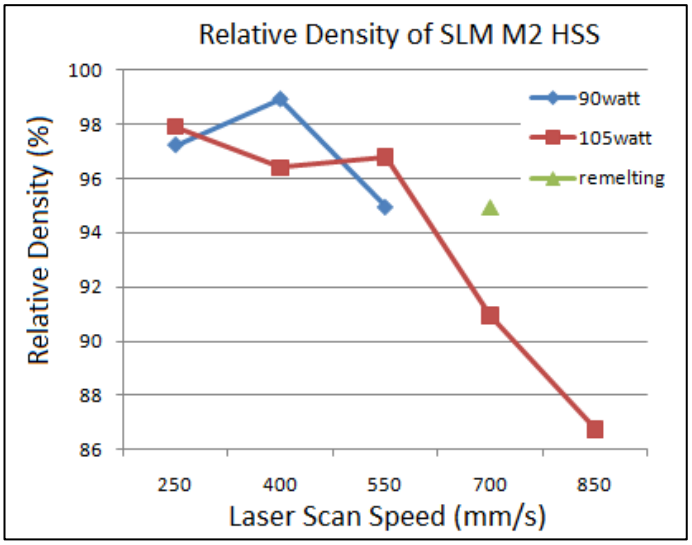

Figure 5. Preliminary density results.

Under LOM, aligned porosity (Figure 6a) can be observed on parts produced with scan speed of 700 mm/s. This suggests that the scan spacing values that were set are not suitable at higher scan speeds because of a smaller scan track width, higher scan track irregularity and discontinuity which resulted from a lower energy input. As shown in Figure 6b, the width of scan tracks decreased with increasing scan speed. This also explains the obtained low density of 91%.

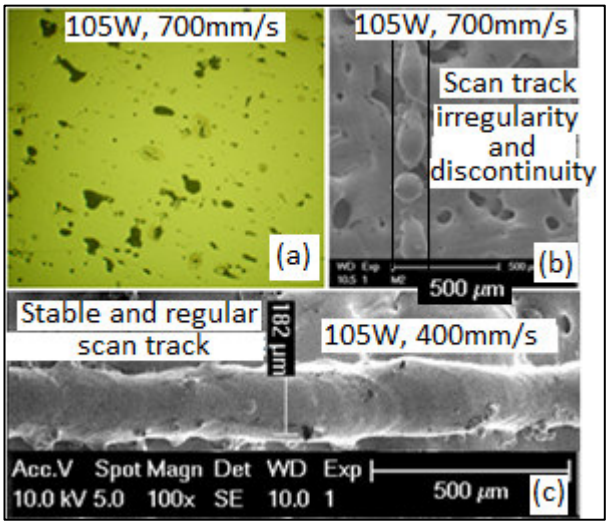

Figure 6. (a) Aligned porosities; (b) scan track irregularity and discontinuity; (c) stable and regular scan track.

3.2 *X-Ray Diffraction (XRD)*

XRD is carried out for three different M2 HSS parts: (1) as cast M2 HSS without heat treatment; (2) SLM produced M2 HSS part and, (3) as supplied M2 HSS virgin powder. These are shown in Figures 7a, 7b and 7c respectively. All 3 graphs look similar under comparison and exhibit the FCC and the BCC phase peaks. It can be seen that the bases of the peaks in Figure 7b are comparatively wider than in Figures 7a and 7c. This suggests that the crystal lattice structures of SLM parts are experiencing certain level of internal stresses that are thermally induced during the rapid solidification SLM process. There is also a shift of the peaks between the as cast and SLM M2 HSS to lower angles suggesting the presence of tensile stresses.

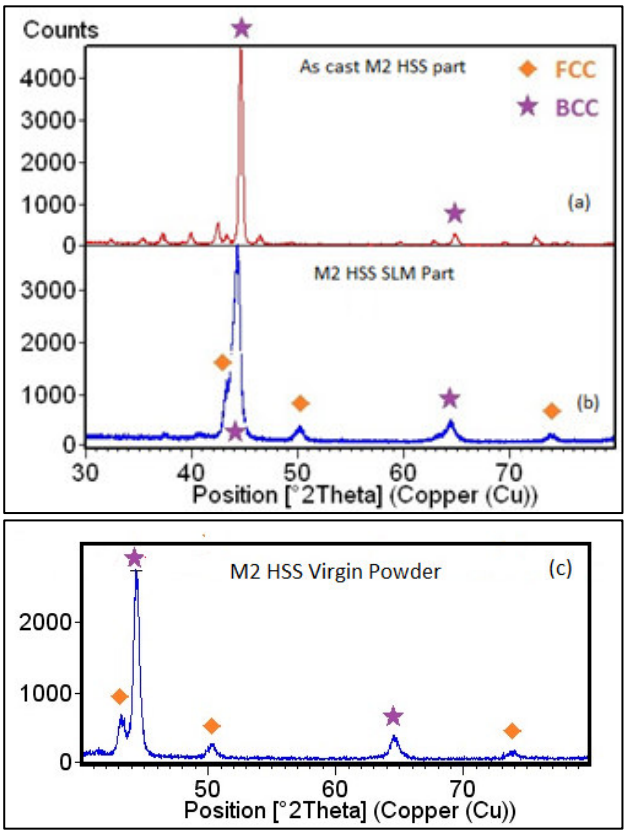

Figure 7. XRD graphs of (a) as cast M2 HSS part without heat treatment; (b) M2 HSS SLM part; (c) as supplied M2 HSS virgin powder from LPW;

Peaks corresponding to expected carbides, $M_{23}C_6$ and M_2C (where M represents V, Cr, Mo or W) in SLM parts are also missing when compared to Figure 8. These are the carbides normally found in M2 HSS parts from similar processes such as laser surface melting (Kac, *et al.* 2003; Arias, *et al.* 2010; Arias, *et al.* 2010). Other types of carbides (MC and M_6C) usually found in annealed and conventionally hardened (Kim, *et al.* 1979) M2 HSS parts, were also not found from three of the XRD tests. Preliminary XRD results also suggested that M2 HSS SLM parts contain 80% martensitic phase and 20% austenitic phase after Rietveld Refinement analysis.

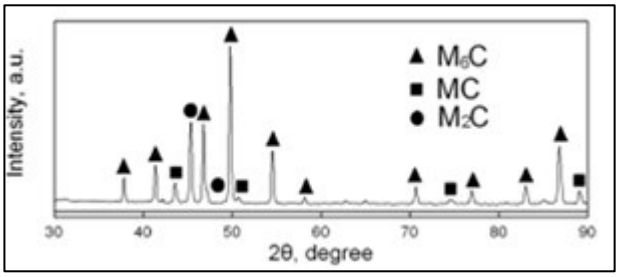

Figure 8. As cast M2 HSS part with controlled cooling rates (Zhou, *et al.* 2010).

3.3 *Microstructure Analysis*

M2 HSS SLM parts (in the y-z plane as illustrated in Figure 9a) were polished till 1 µm and etched with Vilella's reagent for 10 s to review the microstructure. Under LOM (Figure 9b), it can be observed that two distinct phases, a dark and a bright phase are present within every melt pool. Furthermore, parts produced with different scan speed exhibit different percentages of dark and bright phases as compared in Figures 9b and 9c. The percentage bright phase increases with increasing scan speed which can be seen in Figure 9c where the microstructure is dominated by the white phases. This corresponds to the increasing speed of solidification.

Upon close magnification under LOM, bright phases revealed a needle like martensitic structure (Figure 9d) whereas dark phases revealed a dendritic (Figure 9e) and cellular (Figure 9f) like structure with growth direction towards the melt pool center.

At the melt pool boundary, the region shown in Figure 10 is supposed to be the remelted fusion zone. In this fusion zone, solidification of the melt material proceeded spontaneously by the epitaxial growth of remelted grains on the previously solidified material. This solidification morphology is influenced by the cooling rate, thermal gradient and growth velocity as described in welding (David, *et al.* 2003).

The M2 HSS SLM parts were also subjected to Groesbeck reagent to etch for carbides. Under LOM, dark spots (Figure 11) that are suspected to be carbides can be seen along the cellular and dendritic structure which cannot be detected by XRD or SEM-EDS.

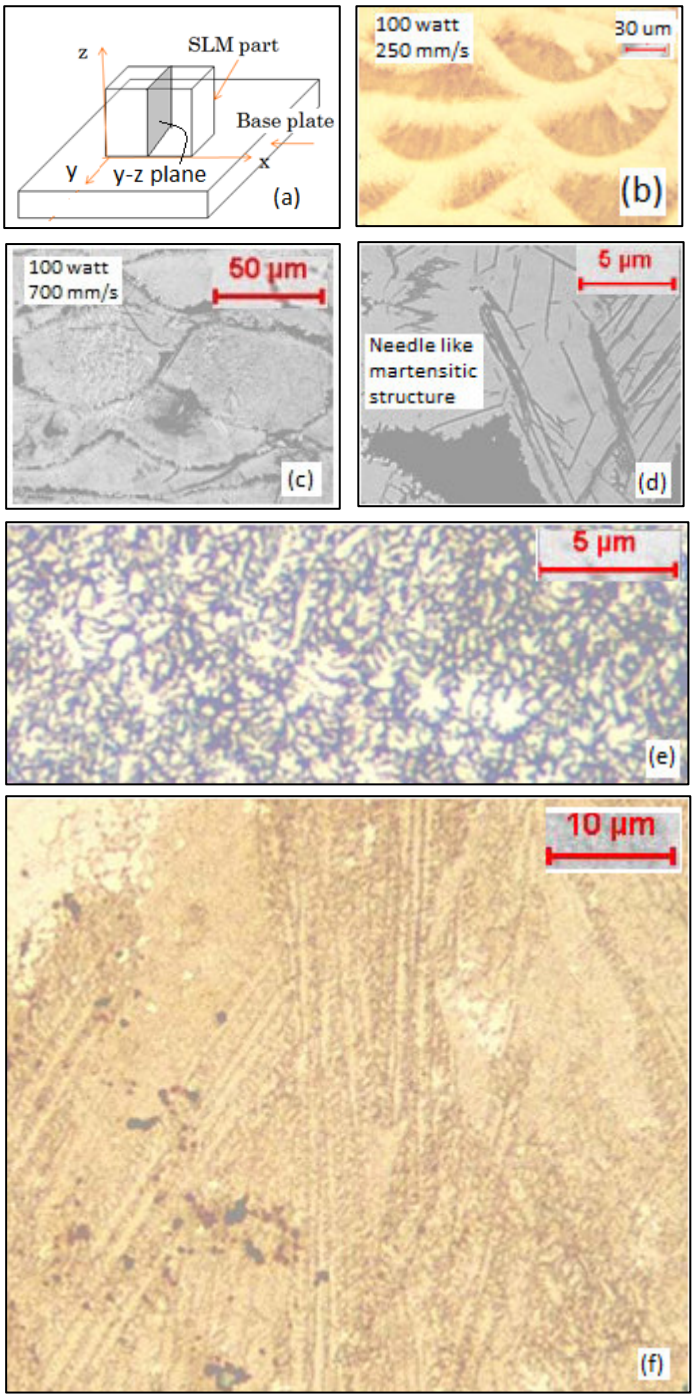

Figure 9. (a) y-z plane illustration; (b) Dark and bright phase microstructure; (c) Dominant bright phase microstructure; (d) Needle-like martensitic structure found in the bright phase; (e) Dendritic structure found in dark phase; (f) Cellular like structure found in dark phase.

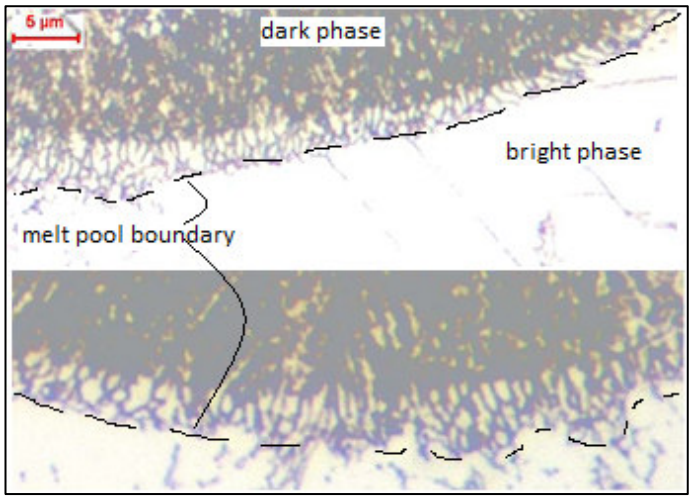

Figure 10. Fusion zones between melt pools showing epitaxial grain growth along the boundaries. Dark phase consisted mainly martensite and ferrite whereas bright phase consisted mainly martensite.

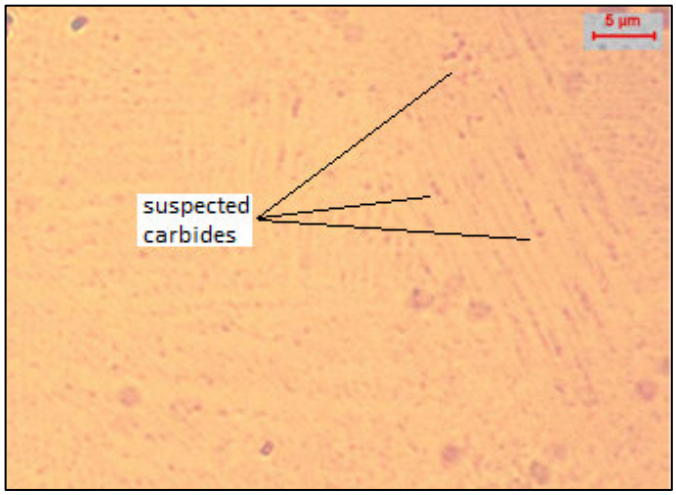

Figure 11. Suspected carbides observed from LOM.

3.4 *Electron Backscatter Diffraction (EBSD)*

In EBSD tests, the dark phases can be indexed. However, the bright phases cannot be indexed and it remains as an unknown phase from the EBSD results. Figure 12 shows the indexed results from a M2 HSS SLM part. The white areas correspond to dark phases with high confidence index (CI) with values ranging from 0.1 to 0.6. The black areas are with low CI. The phase composition was then analyzed with OIM Analysis software version 5.31. The results show that within the dark phase, 45%, 53% and 1% were martensite, ferrite and austenite respectively.

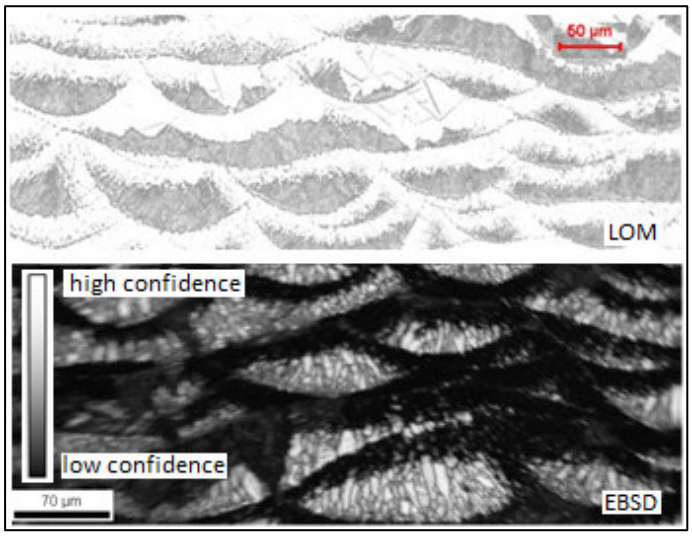

Figure 12. EBSD results showing dark phases (in LOM) being indexed with high confidence level.

3.5 *Coulometry Test*

Coulometry tests were carried out to determine the percentage of carbon content in the M2 HSS after the SLM process. The results show that the carbon content is lower in SLM parts produced with a lower scan speed. Also, the SLM parts show a lower carbon content as compared to the as supplied virgin powder. A supposedly 0.9% C-content in M2 HSS was only 0.7% in the supplied powder and as low as 0.15% in the SLM part. The resolution of this technique is 0.1 ppm, (=0.0001 wt%C) and the reproducibility is about 0.5% relatively.

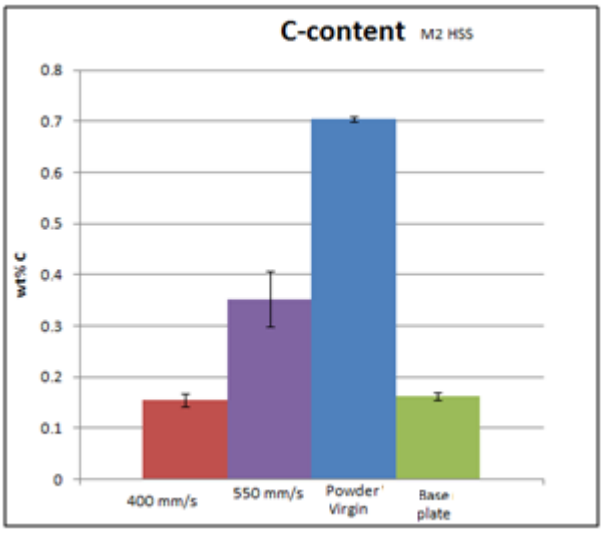

Figure 13. Coulometry test results of M2 HSS.

3.6 *Microhardness Test*

Microhardness tests were carried out on the M2 HSS SLM parts and the results are shown in Figure 14. A load of 100 g was used (Shi, *et al.* 1995; Niu, *et al.* 2000; Benyounis, *et al.* 2009). The results are compared between SLM parts produced with different scanning speeds and they do not show any significant difference. However, measurements taken from the dark and bright phase show a significant difference. As shown in Figure 14b, average hardness for the dark and bright phases was about 700 HV and 870 HV respectively.

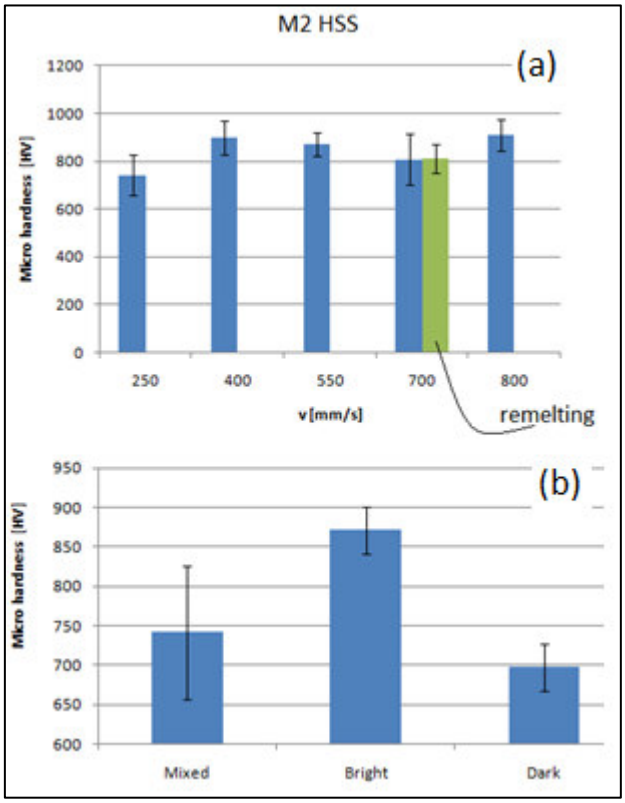

Figure 14. (a) Hardness values of parts produced with different scanning speeds; (b) Hardness values of dark and bright phase.

4 DISCUSSION

In this preliminary investigation, it is observed that cracks are very easily induced in M2 HSS SLM parts. This is probably because M2 HSS is a brittle material owing to its high carbon content compared relatively to AISI 316L SS. The coulumetry results show that parts produced with lower scan speeds have lower carbon content and yet these parts are more prone to crack. This means that the thermal stresses created during the high heat energy input resulting from low scan speeds have more effect than the C-content on inducing cracks.

From the XRD results, no peaks responsible for the carbides can be found in the SLM parts. Coulometry test results also suggested at the carbon content after the SLM process had decreased to as low as 0.15% from 0.7%. However, under LOM observations, black spots that fit the usual carbides segregation description along cellular structures are spotted. These spots are suspected to be the carbides.

There are two reasons why the XRD could not detect carbides. First, the carbon contents are very low and the amount of carbides formed is low. Secondly, due to the quick solidification nature of the SLM process, the dendrites and cells are small and from Figure 10, the sizes of the black spots are extremely small, in the range of 0.1 μm to 0.5 μm. As such, carbide peaks may be too weak to be detected compared to the inherent background noises from the XRD.

The microstructure of M2 HSS SLM parts mainly comprises of dark and bright phases, indicating the melt pools that arose from the SLM building and scanning strategy. From EBSD results, the dark phases consist of mostly ferrite and martensite which explain the average hardness value of 700HV. While the bright phases could not be indexed, LOM and microhardness tests suggest that the bright phases are martensitic as needle-like martensite and high hardness of 800HV is observed and measured respectively. Moreover, the bright phases were in the melt pool locations where the highest cooling rate (which would result in martensite formation) would occur.

Laser re-melting of M2 HSS parts did improve the density significantly by about 3%. Also, microstructure and hardness values of laser re-melted parts remained largely similar. Additionally, surface remelting consistently improved the surface quality by about 2 μm and 3 μm for P_a (unfiltered 2D roughness test) and S_a (3D roughness test) respectively.

5 CONCLUSION AND FUTURE WORK

5.1 *Conclusion*

In conclusion, the SLM of M2 HSS has been proven to be feasible. While base plate separation cannot be fully eliminated in this preliminary investigation, parts without cracks can be produced with an achievable density of 97%. Also in this research, preheating of the base plate was found to have a positive effect on the the parts, minimising cracks and warpage. Furthermore, parts produced directly from the SLM process have high average hardness values between 800 HV to 900 HV which are comparable to conventionally produced cast parts. These conventionally produced M2 HSS cast parts have hardness values between 750 HV to 830 HV depending on the heat treatment process (Davis 1995).

5.2 *Future Work*

The future work aims to address some shortcomings in this research. Firstly, laser re-melting process will be investigated to further improve density values and prevent base plate separation. Currently, surface remelting scanning speed stands at only 700 mm/s. Different scanning speeds can be examined to improve the densities of parts.

Secondly, it was found that preheating of the base plate to 180^{o}C produced better parts (less prone to cracks) compared to a pre-heating of 100^{o}C as the thermal gradient was greatly reduced, thereby inducing less thermal stress. Since 180^{o}C is the preheating limit of the heating system currently installed on the M3 Linear, future modification (within manufacturer specifications) will be carried out to increase the preheating temperature above 180^{o}C. Similar to laser welding, preheating temperatures of 200^{o}C may be applied to reduce the chances of cracking.

Thirdly, the evidence of carbides was not strong enough in this paper. Future work includes SEM and TEM with higher magnification to verify the presence of carbides and to also identify the type of carbides that are present. Additionally, more research can be carried out to understand the reason in the decreasing carbon content.

Lastly, heat treatment process for M2 HSS SLM parts will be optimized. Microstructural studies and material characterization will be carried out to understand the essential difference, between cast and SLM M2 HSS parts. Material properties such as wear resistance, hot hardness and toughness will also be carried out.

6 PREFERENCES

(1997). Weld Integrity and Performance. USA, ASM International.

3DSystems. (2011). "3D Systems." Retrieved March 2010, 2010, from http://www.3dsystems.com/.

Arias, J., *et al.* (2010). "Microstructural characterization of laser surface melted AISI M2 tool steel." Journal of Microscopy-Oxford **239**(3): 184-193.

Arias, J., *et al.* (2010). "Modification of AISI M2 high speed tool steels after laser surface melting under different operation conditions." Revista De Metalurgia **46**(3): 206-218.

Benyounis, K. Y., *et al.* (2009). "Rapid solidification of M2 high-speed steel by laser melting." Materials & Design **30**(3): 674-678.

Bertrand, P., *et al.* (2007). Ceramic components manufacturing by selective laser sintering. Symposium on Laser Synthesis and Processing of Advanced Materials held at the E-MRS 2007 Spring Meeting, Strasbourg, France, Elsevier Science Bv.

Campbell, I. (2009). "The international journal for research on additive manufacturing technologies and rapid product development." Rapid Prototyping Journal **15**(5): 315-315.

Chua, C. K., *et al.* (2010). Rapid Prototyping - Principles and Applications. Singapore, World Scientific Publishing Co. Pte. Ltd.

ConceptLaser. (2011, 16th July 2009). "CONCEPT Laser GmbH." Retrieved September, 2009, from http://www.concept-laser.de/.

David, S., *et al.* (2003). "Welding: Solidification and microstructure." JOM Journal of the Minerals, Metals and Materials Society **55**(6): 14-20.

Davis, J. R. (1995). Tool Materials, ASM International.

Dawes, C. (1992). Laser Welding - A Practical Guide. Cambridge, Abington Publishing.

EOS. (2011). "EOS e-Manufacturing Solutions." Retrieved March 2010, 2010, from http://www.eos.info/en/home.html.

Ion, J. C. (2005). Laser Processing of Engineering Materials: Principles, Procedure and Industrial Application. Burlington, Elsevier Butterworth-Heinemann.

Kac, S., *et al.* (2003). "SEM and TEM microstructural investigation of high-speed tool steel after laser melting." Materials Chemistry and Physics **81**(2-3): 510-512.

Khan, M., *et al.* (2010). "Selective Laser Melting (SLM) of pure gold." Gold Bulletin **43**(2): 114-121.

Kim, Y.-W., *et al.* (1979). "Laser melting and heat treatment of m2 tool steel: A microstructural characterization." Metallurgical and Materials Transactions A **10**(7): 881-886.

Kruth, J. P., *et al.* (2008). Experimental Investigation of Laser Surface Remelting for the Improvement of Selective Laser Melting Process. Proceedings of SFF Symposium, Austin, TX, USA.

Kruth, J. P., *et al.* (2005). Digital manufacturing of biocompatible metal frameworks for complex dental prostheses by means of SLS/SLM. Virtual Modeling and Rapid Manufacturing - Advanced Research in Virtual and Rapid Prototyping. P. J. Bartolo, A. J. Mateus, F. C. Batistaet al. London, Taylor & Francis Ltd**:** 139-145.

Louvis, E., *et al.* (2011). "Selective laser melting of aluminium components." Journal of Materials Processing Technology **211**(2): 275-284.

MTTTechnologies. (2011). "MTT Technologies, Rapid Manufacturing Technologies." Retrieved March 2010, 2010, from http://www.mtt-group.com/.

Mumtaz, K. A., *et al.* (2007). "Laser melting functionally graded composition of Waspaloy((R)) and Zirconia powders." Journal of Materials Science **42**(18): 7647-7656.

Nga, C. C., *et al.* (2011). "Microstructure and mechanical properties of selective laser melted magnesium." Applied Surface Science **257**(17): 7447-7454.

Nga, C. C., *et al.* (2010). "Layer manufacturing of magnesium and its alloy structures for future applications." Virtual and Physical Prototyping **5**(1): 13-19.

Niu, H. J., *et al.* (2000). "Microstructural evolution during laser cladding of M2 high-speed steel." Metallurgical and Materials Transactions a-Physical Metallurgy and Materials Science **31**(10): 2615-2625.

PhenixSystems. (2011, 18th Sep 2009). "Phenix Systems." Retrieved 18th Sep 2009, 2009, from http://www.phenix-systems.com/phenix_en/home.htm.

Shi, G., *et al.* (1995). "Microstructure and properties of laser surface hardened M2 high speed steel." Acta Metallurgica et Materialia **43**(1): 217-223.

Shishkovsky, I., *et al.* (2007). "Alumina-zirconium ceramics synthesis by selective laser sintering/melting." Applied Surface Science **254**(4): 966-970.

Totten, G., *et al.* (2002). Handbook of Residual Stress and Deformation of Steel. Materials Park, Ohio, ASM International.

Vandenbroucke, B., *et al.* (2007). "Selective laser melting of biocompatible metals for rapid manufacturing of medical parts." Rapid Prototyping Journal **13**(4): 196-203.

Wehmoller, M., *et al.* (2005). Implant design and production - a new approach by selective laser melting. CARS 2005: Computer Assisted Radiology and Surgery. H. U. Lemke, K. Inamura, K. Doi, M. W. Vannier and A. G. Farman. Amsterdam, Elsevier Science Bv. **1281:** 690-695.

Yasa, E., *et al.* (2009). Investigation on Occurance of Elevated Edges in Selective Laser Melting. Twentieth Annual International Solid Freeform Fabrication Symposium. Austin, Texas, USA.

Yasa, E., *et al.* (2010). Investigation of Sectoral Scanning in Selective Laser Melting. Biennial ASME Conference on Engineering Systems, Design and Analysis (ESDA) 2010, Istanbul, Turkey.

Zhou, X. F., *et al.* (2010). "A Study on the Microstructure of AISI M2 High Speed Steel Manufactured by Continuous Casting." Advanced Materials Research **146 - 147**: 1211 - 1215.